Coupling of cutoff modes in nonlinear lattices

1999 J. Phys.: Condens. Matter 11 2759

(http://iopscience.iop.org/0953-8984/11/13/012)

J. Phys.: Condens. Matter **11** (1999) 2759–2771. Printed in the UK PII: S0953-8984(99)97112-6

Coupling of cutoff modes in nonlinear lattices

Guoxiang Huang†‡, Peiqing Tong†§ and Bambi Hu†‖

† Department of Physics and Centre for Nonlinear Studies, Hong Kong Baptist University, Hong Kong, People's Republic of China
‡ Department of Physics and Laboratory for Quantum Optics, East China Normal University, Shanghai 200062, People's Republic of China
§ Department of Physics, Nanjing Normal University, Nanjing 210097, People's Republic of China
‖ Department of Physics, University of Houston, Houston, TX 77204, USA

Received 2 September 1998, in final form 4 December 1998

Abstract. The coupling of cutoff modes in nonlinear lattices is considered. It is shown that a novel class of lattice solitons is possible in the form of a coupled soliton–soliton or a coupled kink–soliton pair through a cross-phase modulation. Exact soliton solutions of coupled nonlinear amplitude equations for describing such a type of interacting nonlinear localized mode in lattices are presented and a macro-lattice experiment for their observation is suggested. Analytical results based on a quasi-discreteness approach are checked by numerical simulations.

1. Introduction

The linear elementary excitations in atomic lattices out of ground states, i.e. linear lattice waves or phonons, have been well understood [1]. Due to discreteness the phonon spectrum of a homogeneous linear lattice consists of one band (for monatomic lattices) or several bands (for multi-atomic lattices). Each band is bounded by two cutoff frequencies, which are actually the edges of the band. There is a frequency gap (forbidden band) between two adjacent phonon bands. We call the modes which are related to the cutoff frequencies the cutoff modes of the system. In linear theory, no interaction occurs between phonons and the phonons cannot propagate in forbidden bands.

The study of nonlinear lattice dynamics and related soliton excitations has been greatly influenced by the pioneering works of Fermi *et al* [2] and of Zabusky and Kruskal [3]. Most of the work in this area involved a continuum approximation, which is only valid for a long wavelength, lower cutoff phonon mode. In recent years, the interest in localized excitations in nonlinear lattices has been largely stimulated by the work of Sievers and Takeno [4]. A new type of anharmonic vibrating mode, called the intrinsic localized modes (ILMs) [4, 5] or the discrete breathers [6] has been identified. The ILM is the discrete analogy of an envelope (or breather) soliton with its spatial extension being only a few lattice spacings and the vibrating frequency lying above the phonon band. Its formation is due to the instability of self-phase modulation (SPM) of the corresponding high frequency upper cutoff phonon mode. For diatomic lattices it is shown that an intrinsic gap mode (IGM) may occur [7] and related existence criterion has also been given recently [8, 10]. Experimentally, the ILMs and the IGMs have been observed in coupled pendulum lattices and in electric lattices [11–13].

0953-8984/99/132759+13$19.50

Up to now the nonlinear localized excitations related to the lower and upper phonon modes have been considered separately [4–13]. In this paper we show that in nonlinear lattices there exists a strong interaction between different cutoff modes through a cross-phase modulation (CPM). A novel class of nonlinear localized structures in lattices is found to be possible in the form of coupled soliton–soliton or kink–soliton pairs.

The paper is organized as follows. In the next section, the model is introduced and an asymptotic expansion is made for the lattice equation of motion. The nonlinearly coupled amplitude equations for the cutoff modes of the lattice are derived based on a quasi-discreteness approach (QDA). In section 3 we consider coupled kink–soliton and soliton–soliton solutions of the nonlinear amplitude equations. A linear instability analysis for two cutoff-mode excitations of the lattice is discussed in section 4. In section 5 a numerical simulation is used to check the coupled soliton solutions and the stability analysis given in sections 3 and 4. In section 6 we make a suggestion for observing the coupled soliton excitations in a pendulum lattice. Finally, section 7 contains a summary of our results.

2. Asymptotic expansion

The physical idea of the coupling of cutoff modes obtained does not depend drastically on the type of nonlinear lattice, but, for definiteness and for the sake of simplicity we consider a one-dimensional (1D) monatomic lattice with nearest-neighbour interactions and a nonlinear on-site potential. The equation of motion for the displacement u_n of the nth particle with mass m from its equilibrium position is given by

$$m\ddot{u}_n = k_2(u_{n+1} + u_{n-1} - 2u_n) + k_4[(u_{n+1} - u_n)^3 + (u_{n-1} - u_n)^3] - m\omega_1^2 \sin u_n \tag{1}$$

where k_2 and k_4 are respectively the harmonic and quartic force constants and ω_1^2 is a parameter characteristic of the strength of the on-site potential.

The linear dispersion relation (phonon spectrum) of the system is given by $\omega(q) = [\omega_1^2 + 2(k_2/m)(1 - \cos(qa))]^{1/2}$, where q is wavenumber and ω is frequency. There is a lower cutoff frequency $\omega = \omega_1$ at wavenumber $q = 0$ and a upper cutoff frequency $\omega = \omega_2 = [\omega_1^2 + 4k_2/m]^{1/2}$ at $q = \pi/a$ due to the discreteness of the system, where a is the lattice spacing (see figure 1). We call the mode $q = 0$ with the frequency ω_1 the lower cutoff mode and the

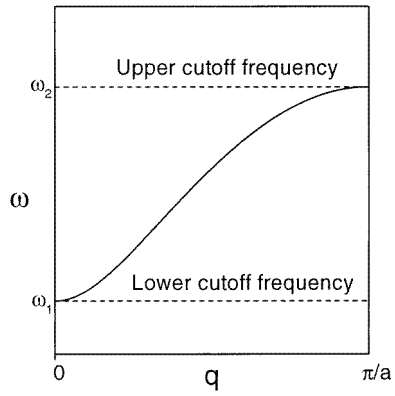

Figure 1. The linear dispersion relation of a one-dimensional monatomic lattice with intersite interaction and nonlinear on-site potential. There is a lower cutoff mode $q = 0$ with the frequency $\omega = \omega_1$ and an upper cutoff mode $q = \pi/a$ with the frequency $\omega = \omega_2 = [\omega_1^2 + 4k_2/m]^{1/2}$.

mode $q = \pi/a$ with the frequency ω_2 the upper cutoff mode. A lot of work has been done on the nonlinear localized excitations related to these two cutoff modes [4–6] but no attention has been paid to their interaction. In fact the interaction exists and may be very strong. The reason for this can be stated as follows: because, for wavepackets with their wavenumbers of carrier waves centred around $q = 0$ or π/a, they have almost equal (i.e. vanishing) group velocities. Thus if two such wavepackets are excited, they will overlap for a very long time if they initially overlapped. Thus a strong interaction between these two wavepackets occurs due to the nonlinearity of the system. The outcome is a formation of coupled nonlinear localized structures through the CPM (see below).

To illustrate the above idea we apply the QDA [9, 10] to solve the nonlinear lattice equation of motion (1). We assume $u_n(t) = \epsilon u_{n,n}^{(1)} + \epsilon^2 u_{n,n}^{(2)} + \epsilon^3 u_{n,n}^{(3)} \ldots$ with $u_{n,n}^{(j)} = u^{(j)}(\xi_n, \tau; \phi_{1,n}(t), \phi_{2,n}(t))$, where ϵ is a small ordering parameter denoting the amplitude of the excitation and $\xi_n = \epsilon(na - \lambda t)$ and $\tau = \epsilon^2 t$ are two multiple-scale (slow) variables. λ is a parameter to be determined by a solvability condition. The 'fast' variables, $\phi_{l,n}(t)(l = 1, 2)$, represent respectively the phases of two carrier waves. The introduction of the multiple-scale variables means the derivative expansion $\mathrm{d}/\mathrm{d}t = \partial/\partial t - \epsilon\lambda\partial/\partial\xi_n + \epsilon^2\partial/\partial\tau$. Using these notations the problem of solving equation (1) is converted into a hierarchy of linear but inhomogeneous equations for $u_{n,n}^{(j)}(j = 1, 2, 3, \ldots)$.

The lowest order solution with the form of two wavepackets is $u_{n,n}^{(1)} = A_1(\xi_n, \tau)\exp[\mathrm{i}\phi_{1,n}(t)] + A_2(\xi_n, \tau)\exp[\mathrm{i}\phi_{2,n}(t)] + \mathrm{CC}$, where $\phi_{l,n}(t) = q_l na - \omega(q_l)t\,(l = 1, 2)$ and $\omega(q)$ is the linear phonon spectrum given above. CC represents corresponding complex conjugate. A_1 and A_2 are two amplitude (or envelope) functions undetermined as yet. To specify two cutoff modes of the system we set $q_1 = 0$ and $q_2 = \pi/a$. Thus we have

$$u_{n,n}^{(1)} = A_1(\xi_n, \tau)\exp(-\mathrm{i}\omega_1 t) + A_2(\xi_n, \tau)(-1)^n \exp(-\mathrm{i}\omega_2 t) + \mathrm{CC} \tag{2}$$

where the first (second) term on the right-hand side corresponds to the lower (upper) cutoff mode. In the next order, a solvability condition requires $\lambda = 0$ thus $\xi_n = \epsilon na$. In fact $\lambda = \mathrm{d}\omega/\mathrm{d}q = [k_2 a/(m\omega)]\sin(qa)$, which vanished for the cutoff modes.

When solving $u_{n,n}^{(3)}$ by two solvability conditions we obtain the coupled nonlinear Schrödinger (NLS) equations for A_1 and A_2

$$2\mathrm{i}\omega_1\frac{\partial A_1}{\partial\tau} + I_2 a^2\frac{\partial^2 A_1}{\partial\xi_n^2} + 3\beta[|A_1|^2 + 2|A_2|^2]A_1 = 0 \tag{3}$$

$$2\mathrm{i}\omega_2\frac{\partial A_2}{\partial\tau} - I_2 a^2\frac{\partial^2 A_2}{\partial\xi_n^2} + 3\beta\left[2|A_1|^2 + \left(1 - \frac{16I_4}{\beta}\right)|A_2|^2\right]A_2 = 0 \tag{4}$$

where $I_j = k_j/m(j = 2, 4)$ and $\beta = \omega_1^2/6$. The different signs of the second-order spatial derivatives result from the different dispersion (denoted by $\omega''(q)$) of the lower and upper cutoff modes. In fact, from the phonon spectrum obtained above, we have $\omega''(0) = I_2 a^2/\omega_1$ and $\omega''(\pi/a) = -I_2 a^2/\omega_2$. Notice that the nearest-neighbour interaction (represented by I_4) makes no contribution to the SPM (denoted by $|A_j|^2 A_j$, $j = 1, 2$) of the lower cutoff mode. This is because, for the lower cutoff mode, the motion of particles is always in phase. For each mode, in addition to the SPM term there exists a CPM term denoted by $|A_j|^2 A_{3-j}$ $(j = 1, 2)$, which will drastically change the property of the nonlinear localized excitations in comparison with the case of a single lower or upper cutoff mode being excited separately.

Let $(v, w) = \epsilon(A_1, A_2)$ and notice that $\xi_n = \epsilon na$ and $\tau = \epsilon^2 t$; we can rewrite the amplitude equations (3) and (4) in the form

$$\mathrm{i}\frac{\partial v}{\partial t} + g_v\frac{\partial^2 v}{\partial x^2} + p_v(|v|^2 + 2|w|^2)v = 0 \tag{5}$$

$$\mathrm{i}\frac{\partial w}{\partial t} - g_w\frac{\partial^2 w}{\partial x^2} + p_w(2|v|^2 + \sigma_w|w|^2)w = 0 \tag{6}$$

where $x = na$, $g_v = I_2a^2/(2\omega_1)$, $g_w = I_2a^2/(2\omega_2)$, $p_v = \omega_1/4$, $p_w = \omega_1^2/(4\omega_2)$ and $\sigma_w = 1 - 96k_4/(m\omega_1^2)$. Obviously, g_v, g_w, p_v and p_w are positive but σ_w may be either sign depending on the strength ratio between the nearest-neighbour interaction and the on-site potential.

3. Coupled soliton solutions

The nonlinear amplitude equations obtained in the last section are different from the ones obtained by Kivshar *et al* when considering the coupling between the counterpropagating lattice waves with the same frequency [14]. In our case the dispersion terms for the lower and the upper modes have different signs and the coefficients of the SPM terms for the two modes are different. These features make the nonlinear coupled localized excitations with different oscillating frequency have quite different properties, which can be seen below.

3.1. Single-mode excitations

Let us first consider single-mode solutions of equations (5) and (6). A lower cutoff mode excitation corresponds to taking $w = 0$ and $v \neq 0$. Thus (5) and (6) are reduced to the NLS equation for v:

$$\mathrm{i}\frac{\partial v}{\partial t} + g_v\frac{\partial^2 v}{\partial x^2} + p_v|v|^2 v = 0 \tag{7}$$

which admits the soliton solution

$$v = \left(\frac{2g_v}{p_v}\right)^{1/2} K\,\mathrm{sech}(Kx - 2g_vKK_1t)\exp\{\mathrm{i}[K_1x - g_v(K_1^2 - K^2)t]\} \tag{8}$$

with K and K_1 being two free parameters. In leading order approximation the lattice displacement takes the form

$$u_n(t) = 2\left(\frac{2g_v}{p_v}\right)^{1/2} K\,\mathrm{sech}(Kna - 2g_vKK_1t)\cos\{K_1na - [\omega_1 + g_v(K_1^2 - K^2)]t\}. \tag{9}$$

For single-mode excitations, it is *impossible* to obtain a kink for the lower cutoff mode.

The upper cutoff mode excitations correspond to setting $v = 0$ and $w \neq 0$. Hence equations (5) and (6) are simplified to the NLS equation for w:

$$\mathrm{i}\frac{\partial w}{\partial t} - g_w\frac{\partial^2 w}{\partial x^2} + p_w\sigma_w|w|^2 w = 0. \tag{10}$$

In this case the type of soliton solution is *mass dependent*. When $m > m_{c,1} = 96k_4/\omega_1^2$ (i.e. $\sigma_w > 0$), we have the kink solution

$$w = \left(\frac{2g_w}{\sigma_w p_w}\right)^{1/2} K\tanh(Kx + 2g_wKK_2t)\exp\{\mathrm{i}[K_2x + g_w(K_2^2 + 2K^2)t]\} \tag{11}$$

with K and K_2 being two free parameters. However, if $m < m_{c,1}$ (i.e. $\sigma_w < 0$), the solution changes into the soliton:

$$w = \left(\frac{-2g_w}{\sigma_w p_w}\right)^{1/2} K\,\mathrm{sech}(Kx + 2g_wKK_2t)\exp\{\mathrm{i}[K_2x + g_w(K_w^2 - K^2)t]\}. \tag{12}$$

The lattice configuration corresponding the solution (12) is given by

$$u_n(t) = (-1)^n 2\left(\frac{-2g_w}{\sigma_w p_w}\right)^{1/2} K \operatorname{sech}(Kx + 2g_w K K_2 t)\cos\{K_2 na - [\omega_2 + g_w(K^2 - K_2^2)t]\}. \tag{13}$$

When K_2 is set to zero, the nonlinear localized excitation expressed in (13) is just the ILM with the oscillating frequency above the phonon band, discussed widely in the literature [4–6].

From the results obtained above we have the conclusion that, for any particle mass, the lower cutoff mode excitation is *always* a soliton, but the upper cutoff excitation may be a soliton or a kink, depending on $m < m_{c,1}$ or $m > m_{c,1}$. However, this picture will be changed when the interaction of the lower and upper cutoff modes is considered.

3.2. Coupled-mode excitations

We are interested in *coupled*-mode excitations of the system. This requires us to solve the coupled nonlinear amplitude equations (5) and (6) with $v \neq 0$ and $w \neq 0$. We find that equations (5) and (6) admit the following coupled soliton solutions, dependent on the particle mass m.

(1) $m > m_{c,2} = 32k_4/\omega_1^2$. In this case we obtain the coupled lower cutoff kink and upper cutoff soliton solution

$$v = V_0 \tanh(Kx - 2g_v K K_1 t)\exp[\mathrm{i}(K_1 x - \Omega_1 t)] \tag{14}$$

$$w = W_0 \operatorname{sech}(Kx + 2g_w K K_2 t)\exp[\mathrm{i}(K_2 x - \Omega_2 t)] \tag{15}$$

with

$$V_0^2 = \frac{2K^2}{4 - \sigma_w}\left(\sigma_w \frac{g_v}{p_v} + 2\frac{g_w}{p_w}\right) \tag{16}$$

$$W_0^2 = \frac{2K^2}{4 - \sigma_w}\left(2\frac{g_v}{p_v} + \frac{g_w}{p_w}\right) \tag{17}$$

$$\Omega_1 = g_v(2K^2 + K_1^2) - 2p_v W_0^2 \tag{18}$$

$$\Omega_2 = g_w(K^2 - K_2^2) - 2p_w V_0^2 \tag{19}$$

where $K_2 = -(g_v/g_w)K_1$ and K, K_1 are two free parameters.

Different for the single-mode excitation discussed in the last subsection, here the lower-cutoff mode is *not* a soliton but a kink! The lattice displacement for the above two-cutoff-mode excitation takes the form

$$u_n(t) = 2V_0 \tanh(Kna - 2g_v K K_1 t)\cos[K_1 na - (\omega_1 + \Omega_1)t] + 2(-1)^n W_0 \operatorname{sech}(Kna + 2g_w K K_2 t)\cos[K_2 na - (\omega_2 + \Omega_2)t]. \tag{20}$$

If K_1 and thus K_2 are set to zero, the excitation denoted by (20) is a *standing* kink–soliton pair.

(2) $m < m_{c,2} = 32k_4/\omega_1^2$. In this case we have the coupled soliton–soliton solution

$$v = V_0 \operatorname{sech}(Kx - 2g_v K K_1 t)\exp[\mathrm{i}(K_1 x - \Omega_1 t)] \tag{21}$$

$$w = W_0 \operatorname{sech}(Kx + 2g_w K K_2 t)\exp[\mathrm{i}(K_2 x - \Omega_2 t)] \tag{22}$$

with

$$V_0^2 = \frac{2K^2}{\sigma_w - 4}\left(\sigma_w \frac{g_v}{p_v} + 2\frac{g_w}{p_w}\right) \tag{23}$$

$$W_0^2 = \frac{2K^2}{4 - \sigma_w}\left(2\frac{g_v}{p_v} + 2\frac{g_w}{p_w}\right) \tag{24}$$

$$\Omega_1 = g_v(K_1^2 - K^2) \tag{25}$$

$$\Omega_2 = g_w(K^2 - K_2^2) \tag{26}$$

where $K_2 = -(g_v/g_w)K_1$ and K and K_1 are still free parameters. The lattice configuration in this case is given by

$$u_n(t) = 2V_0 \operatorname{sech}(Kna - 2g_v K K_1 t)\cos[K_1 na - (\omega_1 + \Omega_1)t] + 2(-1)^n W_0 \operatorname{sech}(Kna + 2g_w K K_2 t)\cos[K_2 na - (\omega_2 + \Omega_2)t]. \tag{27}$$

From the results obtained above we see that for the coupled-mode excitations the upper cutoff mode is always a soliton, but the type of the lower cutoff mode may be a kink or a soliton, controlled by the particle mass $m > m_{c,2}$ or $m < m_{c,2}$. This is different from the case of the single-mode excitations where the lower cutoff mode is always a soliton but the upper cutoff mode may be a soliton or a kink, determined by $m > m_{c,1}$ or $m < m_{c,1}$. Note that the two 'critical masses' $m_{c,1}$ and $m_{c,2}$ are different.

4. Modulational stability analysis

The formation of the coupled kink–soliton and soliton–soliton pairs given in the last section, in particular the lower cutoff kink which is *impossible* for the single-mode excitation, is due to the CPM of the system. To show this one can investigate the modulational instability (MI) of the two-cutoff-mode excitation with the form $u_n(t) = v_0 \exp(-\mathrm{i}\Omega_1 t) + (-1)^n w_0 \exp(-\mathrm{i}\Omega_2 t) + \mathrm{CC}$, where $\Omega_1 = \omega_1 + p_v(v_0^2 + 2\omega_0^2)$ and $\Omega_2 = \omega_2 + p_w(\sigma_w w_0^2 + 2v_0^2)$ with v_0 and w_0 being two real constants, by starting from equation (1). It is well known that the study of stability by using nonlinear amplitude equations has been widely employed in pattern formation in systems outside equilibrium [15, 16]. By a similar idea in the following we shall make a simple discussion for a linear MI analysis of the two-cutoff-mode excitations by using the nonlinear amplitude equations (5) and (6).

Consider the uniform vibrating solution of equations (5) and (6) $v = v_0 \exp(\mathrm{i}\lambda_1 t)$, $w = w_0 \exp(\mathrm{i}\lambda_2 t)$ with $\lambda_1 = p_v(v_0^2 + 2w_0^2)$ and $\lambda_2 = p_w(2v_0^2 + \sigma_w w_0^2)$, which corresponds to extended lower and upper cutoff modes excited simultaneously in the system. Assume that a perturbation is added to the solution, i.e.

$$v = [v_0 + a_1(x,t)]\exp(\mathrm{i}\lambda_1, t) \tag{28}$$

$$w = [w_0 + a_2(x,t)]\exp(\mathrm{i}\lambda_2, t) \tag{29}$$

where $a_j (j = 1, 2)$ are small quantities. Substituting (28) and (29) into equations (5) and (6) and keeping only the linear terms, we obtain

$$\mathrm{i}\frac{\partial a_1}{\partial t} + g_v\frac{\partial a_1}{\partial x^2} + p_v[v_0^2(a_1 + a_1^*) + 2v_0 w_0(a_2 + a_2^*)] = 0 \tag{30}$$

$$\mathrm{i}\frac{\partial a_2}{\partial t} - g_w\frac{\partial a_2}{\partial x^2} + p_w[\sigma_w w_0^2(a_2 + a_2^*) + 2v_0 w_0(a_1 + a_1^*)] = 0. \tag{31}$$

Since any perturbation can be decomposed into normal modes, we assume

$$a_1 = V_1\cos(Kx - \Omega t) + \mathrm{i}V_2\sin(Kx - \Omega t) \tag{32}$$

$$a_2 = W_1\cos(Kx - \Omega t) + \mathrm{i}W_2\sin(Kx - \Omega t) \tag{33}$$

where K and Ω are respectively the wavenumber and frequency of the perturbation and V_j and W_j $(j = 1, 2)$ are small real constants. Substituting (32) and (33) into equations (30) and (31) we obtain a set of linear equations in V_j and W_j. A solvability condition for solving V_j and W_j results in

$$(\Omega^2 + h_1)(\Omega^2 - h_2) + C = 0 \tag{34}$$

where $h_1 = g_v K^2(2p_v v_0^2 - g_v K^2)$, $h_2 = g_w K^2(2\sigma_w p_w w_0^2 + g_w K^2)$ and $C = 16\, p_v p_w g_v g_w v_0^2 w_0^2 K^4$. From equation (34) we have

$$\Omega^2 = (1/2)\{h_2 - h_1 \pm [(h_2 - h_1)^2 + 4(h_1 h_2 - C)]^{1/2}\}. \tag{35}$$

The stability of the uniform vibrating solution is governed by equation (35). If the frequency Ω has a positive imaginary part, the perturbation will grow exponentially thus the solution is unstable. This unstable growth of the perturbation refers to MI. The MI regime is dependent on the parameters v_0, w_0 and the wavenumber K if the system parameters (i.e. g_v, g_w, p_v, p_w and σ_w) are fixed. Here for simplicity we consider the case $(h_2 - h_1)^2 + 4(h_1 h_2 - C) \geqslant 0$, which means $K \leqslant K_1$ with $K_1 = [2\alpha w_0^2(\sigma_w \beta^2 + \gamma^2 - 4\beta\gamma)/(1-\beta^2)]^{1/2}$, where $\alpha = p_v/g_v$, $\beta = g_w/g_v$ and $\gamma = v_0/w_0$. From (35) we see that the Ω_- mode (corresponding to the lower sign of equation (35)) firstly becomes unstable. The growth rate is given by $\sigma_r = \mathrm{Im}\,\Omega_-$, i.e.

$$\sigma_r = \frac{1}{\sqrt{2}}\{[(h_2 - h_1)^2 + 4(h_1 h_2 - C)]^{1/2} - (h_2 - h_1)\}^{1/2}. \tag{36}$$

For $K_0 \leqslant K < K_1$ (i.e. $h_1 \leqslant h_2$), where $K_0 = [2\alpha w_0^2(\gamma^2 - \sigma_w \beta^2)/(1+\beta^2)]^{1/2}$, the necessary condition for the MI to occur is $h_1 h_2 - C > 0$, i.e.

$$K_0 \leqslant K < K_+ \leqslant K_1 \tag{37}$$

where

$$K_+ = \sqrt{\alpha} w_0 \{\gamma^2 - \sigma_w + [(\gamma^2 - \sigma_w)^2 - 4(4 - \sigma_w)\gamma^2]^{1/2}\}^{1/2}. \tag{38}$$

For $0 < K < K_0$ (i.e. $h_1 > h_2$), σ_r is always positive thus the uniform vibrating solution is unstable. $K = 0$ and $K = K_+$ are critical wavenumbers of the instability, i.e. $\sigma_r(K = 0) = \sigma_r(K = K_+) = 0$. Shown in figure 2 is the growth rate σ_r of the perturbation for several values of γ after taking $w_0 = 0.005$. (Since the growth rate is symmetric with $\sigma_r(-K) = \sigma_r(K)$, only the positive-wavenumber part is shown.)

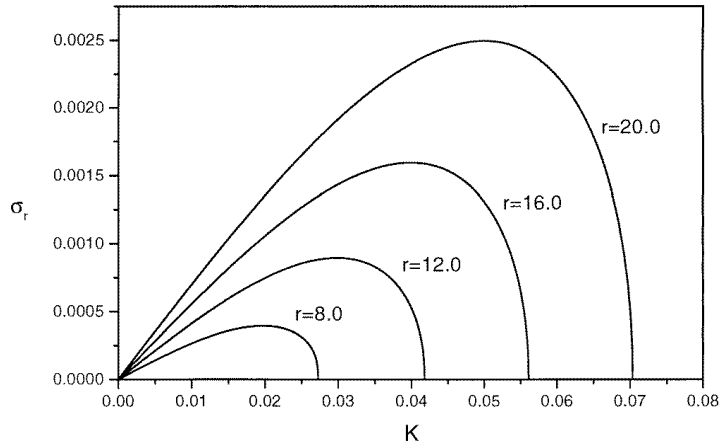

Figure 2. Growth rate $\sigma_r(K)$ for several values of γ after taking $w_0 = 0.005$. Only half of the spectrum is shown since $\sigma_r(-K) = \sigma_r(K)$. The system parameters chosen in the figure are $\alpha = p_v/g_v = 0.25$, $\beta = g_w/g_v = 0.33$ and $\sigma_w = -3.8$.

From the discussion given above, we see that the MI involves two amplitude parameters, v_0 and w_0. This is just the CPM which implies that there is a nonlinear phase change of the lower cutoff mode induced by the upper cutoff mode, and vice versa. At a later stage of the

stability the exponential growth of the perturbation in the unstable region will be balanced by the nonlinearity of the system. The nonlinearly coupled localized structures given in equations (20) and (27) are just the results of the CPM. This explains why the lower cutoff kink given in (14) is possible for a coupled-mode but not for a single-mode excitation. The CPM in plasma physics and in nonlinear optics has been discussed by Berkhoer and Zakharov [17] and Agrawal [18].

5. Numerical simulations

In this section we use a molecular-dynamics simulation to test the analytical results obtained in the last two sections. Taking the analytical soliton solutions as initial conditions, we investigate the time evolution of the system by numerically integrating the lattice equation of motion (1), using the fourth order Runge–Kutta method. Since there exist published numerical results for a single lower or upper cutoff nonlinear excitation [4–6], here we present only the numerical results of the nonlinear coupled modes given in section 3.2. We found that these nonlinearly coupled localized modes are quite long lived. They can last for at least one hundred time units. In general, the lifetime is longer for the excitations with smaller amplitudes.

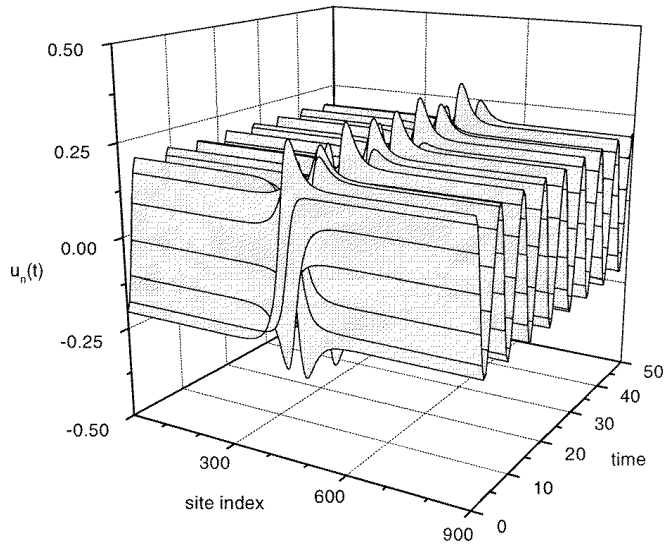

Figure 3. The time evolution of the kink–soliton excitation corresponding to the lower and upper cutoff modes for $m > m_{c,2} = 32k_4/\omega_1^2$. The parameters are chosen as $N = 900$, $m = a = \omega_1 = 1.0$, $k_2 = 2.0$, $k_4 = 0.01$, $K = 0.05$ and $K_1 = 0$.

As examples, in figures 3 and 4 we have shown the time evolution of two types of coupled-mode excitation. In our numerical simulation, we chose a chain of $N = 900$ particles with appropriate boundary conditions. In the regime $m > m_{c,2} = 32k_4/\omega_1^2$, the lower cutoff mode is a kink and the upper cutoff mode is a soliton. Shown in figure 3 is the time evolution for the coupled lower cutoff kink and upper cutoff soliton mode, taking (20) as an initial condition. Since the lower cutoff mode is a kink, we cannot impose a periodic boundary condition. Instead, we use an absorbing boundary condition by assuming two imaginary particles at each end of the chain. These imaginary particles play the role of absorbing waves from the bulk of the chain and preventing the reflection of waves from the boundaries into the bulk. We

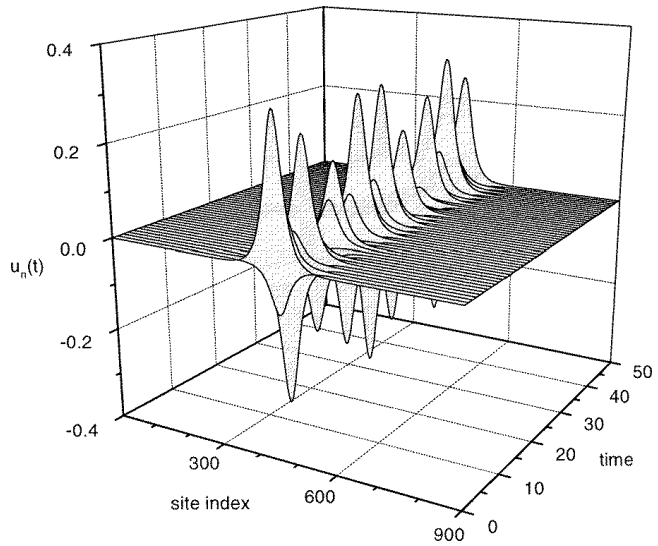

Figure 4. The time evolution of the kink–soliton excitation corresponding to the lower and upper cutoff modes for $m > m_{c,2} = 32k_4/\omega_1^2$. The parameters are chosen as $N = 900$, $m = a = \omega_1 = 1.0$, $k_2 = 2.0$, $k_4 = 0.01$, $K = 0.05$ and $K_1 = 0$.

also check the results by using pseudo-periodic boundary condition but no difference has been found. The parameters K and K_1 of figure 3 are respectively taken as 0.05 and zero. From figure 3, we see that the lattice displacement is basically the superposition of a kink and a soliton but there is an oscillation following time. The numerical simulation shows that such a coupled kink–soliton solution is very stable and long lived. For nonzero K_1, the coupled kink–soliton mode has nonzero velocity. Since there exists a spatially periodic oscillation factor in the lattice displacement, the evolution pattern of the solution in this case is a little complex.

In the regime $m < m_{c,2}$, we have a coupled soliton–soliton solution. By taking (27) as an initial condition and using a period boundary condition, we obtain the evolution pattern of the solution following time, which is shown in figure 4. The coupled soliton–soliton solution is also very stable and long lived.

In order to check our analytical results from the modulational stability of extended lower and upper cutoff modes, given in the last section, we have also numerically studied the time evolution of the extended two-cutoff-mode excitation $u_n(t) = v_0 \exp(\mathrm{i}\lambda_1 t) + (-1)^n w_0 \exp(\mathrm{i}\lambda_2 t) + \mathrm{CC}$ (where λ_1 and λ_2 have been given in the last section) in different parameter regimes when a linear perturbation is added in the way $v_0 \to v_0 + a_1$, $w_0 \to w_0 + a_2$ with $a_1 = V_1 \cos(Kna - \Omega t) + \mathrm{i}V_2 \sin(Kna - \Omega t)$ and $a_2 = W_1 \cos(Kna - \Omega t) + \mathrm{i}W_2 \sin(Kna - \Omega t)$. We also superpose a random noise on the initial velocity. Shown in figures 5(a) and (b) are the snapshots of the energy density distribution of the system, defined by

$$e_n(t) = \frac{1}{2}m\left(\frac{\mathrm{d}u}{\mathrm{d}t}\right)^2 + \frac{k_2}{4}[(u_{n-1} - u_n)^2 + (u_{n+1} - u_n)^2] + \frac{k_4}{8}[(u_{n-1} - u_n)^4 + (u_{n+1} - u_n)^4] + m\omega_1^2(1 - \cos u_n) \tag{39}$$

at different time. The results are obtained for $N = 900$ with a periodic boundary condition. The magnitude of the random noise is $V_n = 0.03$. In figure 5(a), the wavenumber of the

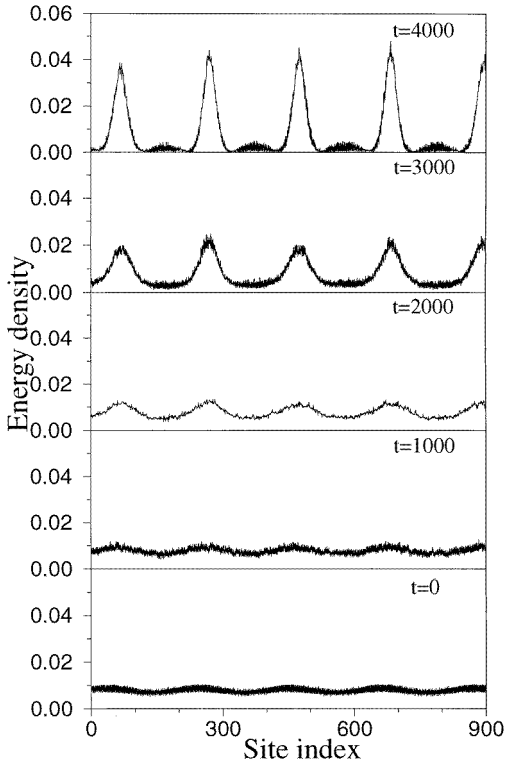

(a)

Figure 5. The modulational instability of the extended lower and upper cutoff modes. The snapshots of the energy density distributions are determined by molecular-dynamics simulations for the extended lower and upper cutoff modes with perturbations in the chain containing 900 particles with a periodic boundary condition. (a) The parameter $K = 0.03$ is inside the unstable parameter region; (b) the parameter $K = 0.042$ is outside the unstable parameter region. For both cases $\gamma = 12.0$. We also superpose a random noise on the initial velocity and the magnitude of noise is $V_n = 0.03$.

perturbation $K = 0.03$ is inside the unstable parameter region of the modulational instability, i.e. $0 < K < K_+$, while in figure 5(b) $K = 0.042$ is outside the unstable parameter region $K > K_+$, where $\gamma = 12.0$ and K_+ has been given in equation (38). The initial conditions are chosen as $V_1 = V_2 = 0.003$, $W_1 = W_2 = 0.001$, $v_0 = 0.06$ and $w_0 = 0.005$. The behaviours of the two cases are quire different. For the chain with K outside the unstable region (figure 5(b)), the energy density remains spatially extended throughout the whole simulation time. However, figure 5(a) demonstrates that the extended lower and upper cutoff mode are unstable for K inside the unstable region. As a consequence of the modulational instability the extended lower and upper cutoff modes evolve into localized structures. This process provides a possible mechanism for the formation of the coupled kink–soliton and soliton–soliton excitations in the system.

6. Coupled modes in a pendulum lattice

Although up to now there have been a lot of theoretical studies on the nonlinear localized excitations (ILMs, IGMs etc) in lattice systems [5, 6], a physical observation for such

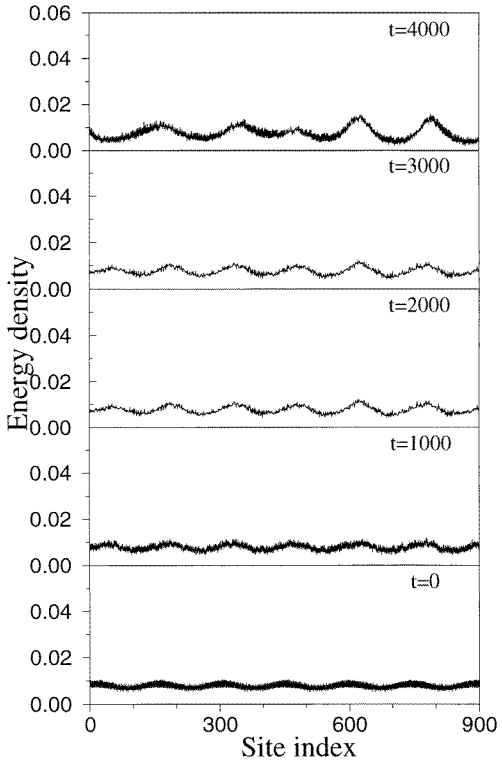

(b)

Figure 5. (Continued)

excitations in atomic lattices is still absent. However, as a first step, we can use some macro-lattices like pendulum and electric lattices [11–13] to examine the theoretical prediction. The dynamics of the coupled modes in nonlinear lattices given above can be tested by a pendulum lattice experiment. Not long ago both the nonlinear upper and lower cutoff modes in a damped and parametrically driven pendulum lattice were separately observed [11, 19]. One can use the same apparatus to observe the coupled soliton–soliton and kink–soliton pairs presented above. To excite two modes we can apply in the vertical direction an external double frequency drive $z_0(t) = -A_{e1}\cos(2\omega_{e1}t) - A_{e2}\cos(2\omega_{e2}t)$, where ω_{e1} and ω_{e2} are near the lower cutoff frequency ω_1 and the upper cutoff frequency ω_2 of the pendulum lattice, respectively. The equation of motion of the pendulum lattice is

$$ml\ddot{\theta}_n = k_2 l(\theta_{n+1} + \theta_{n-1} - 2\theta_n) + k_4 l^3[(\theta_{n+1} - \theta_n)^3 + (\theta_{n-1} - \theta_n)^3] \\ -m(g + \ddot{z}_0)\sin\theta_n - \beta_0 l\dot{\theta}_n \tag{40}$$

where θ_n is the angle displacement of the nth pendulum in the transverse direction of the lattice. m and l are the mass and length of each pendulum, respectively. g is the gravity acceleration and β_0 is the damping coefficient. For details of the model, see [11, 12] and [19]. The occurrence of the cubic term in the right-hand side of the above equation is due to the nonlinear inter-site interaction between adjacent pendulums, see [11] and [12].

Again using the QDA and taking the expansion $\theta_n(t) = \sum_{j=1}\epsilon^j\theta_{n,n}^{(j)}$ with $\theta_{n,n}^{(1)} = A_1(\xi_n, \tau)\exp(-\mathrm{i}\omega_1 t) + A_2(\xi_n, \tau)\exp(-\mathrm{i}\omega_2 t) + \mathrm{CC}$, we obtain the following modified coupled

NLS equations

$$\mathrm{i}\frac{\partial v}{\partial t} + g_v \frac{\partial^2 v}{\partial x^2} + p_v(|v|^2 + 2|w|^2)v + \mathrm{i}(\gamma_0/2)v - d_v v^* = 0 \tag{41}$$

$$\mathrm{i}\frac{\partial w}{\partial t} - g_w \frac{\partial^2 w}{\partial x^2} + p_w(2|v|^2 + \sigma_w|w|^2)v + \mathrm{i}(\gamma_0/2)w - d_w w^* = 0 \tag{42}$$

when returning to the original variables. In deriving the above equations we have assumed that the damping and drive are of order ϵ^2 thus we have $4(\omega_{ej})^2 A_{ej}/g = \epsilon^2\eta_{0j}$ $(j = 1, 2)$ and $\beta_0/m = \epsilon^2\gamma_0$ with η_{0j}, γ_0 being constants of order unity. In equations (41) and (42) $d_v = \eta_{01}\omega_1/4, d_w = \eta_{02}\omega_1^2/(4\omega_2)$ and $(v, w) = \epsilon(A_1 \exp[\mathrm{i}(\omega_1 - \omega_{e1})t], A_2 \exp[\mathrm{i}(\omega_2 - \omega_{e2})t])$. The definitions of g_v, g_w, p_v and p_w are the same as in equations (5) and (6) but here $\omega_w = 1 - 96K_4 l^3/(mg)$. The last two terms in equations (41) and (42) represent the damping and drive, respectively.

It is striking that equations (41) and (42) still admit coupled kink–soliton and soliton–soliton solutions. If $m > m_{c,3} = 32k_4 l^3/g$, we have $v = V_0 \tanh(Kx)\exp(-\mathrm{i}\phi_1)$ and $w = W_0 \operatorname{sech}(Kx)\exp(-\mathrm{i}\phi_2)$, where $V_0^2 = 2K^2(\sigma_w g_v/p_v + 2g_w/p_w)/(4 - \sigma_w)$, $W_0^2 = 2K^2(2g_v/p_v + g_w/p_w)/(4 - \sigma_w)$, $\sin 2\phi_1 = \gamma_0/(2d_v)$ and $\sin 2\phi_2 = \gamma_0/(2d_w)$. Thus it is a coupled *standing kink–soliton* pair and K is no longer a free parameter but determined by $K_2 = (4 - \sigma_w)d_v \cos 2\phi_1/[2(\sigma_w g_v + 2p_v g_w/p_w)]$. The lattice configuration in the leading order approximation is

$$\theta_n(t) = 2V_0 \tanh(Kna)\cos(\omega_1 t + \phi_1) + 2(-1)^n W_0 \operatorname{sech}(Kna)\cos(\omega_2 t + \phi_2). \tag{43}$$

When $m < m_{c,3}$ we obtain the *standing soliton–soliton* solution $v = V_0 \operatorname{sech}(Kx)\exp(-\mathrm{i}\phi_1)$ and $w = W_0 \operatorname{sech}(Kx)\exp(-\mathrm{i}\phi_2)$, where $V_0^2 = 2K^2(\sigma_w g_v/p_v + 2g_w/p_w)/(\sigma_w - 4)$, $W_0^2 = 2K^2(2g_v/p_v + g_w/p_w)/(4 - \sigma_w)$ and $K^2 = d_v \cos 2\phi_1/g_v$. The values of ϕ_1 and ϕ_2 are the same as above. The lattice configuration for this case takes the form

$$\theta_n(t) = 2V_0 \operatorname{sech}(Kna)\cos(\omega_1 t + \phi_1) + 2(-1)^n W_0 \operatorname{sech}(Kna)\cos(\omega_2 t + \phi_2). \tag{44}$$

The above results show that, using the pendulum lattice with a double-frequency drive, one can observe not only the formation of coupled nonlinear localized structures but also the dynamical 'phase transition' from a coupled kink–soliton pair to a soliton–soliton pair by changing the mass or length of the pendulum.

7. Discussion and summary

We have investigated the coupling of the lower and upper cutoff modes in a monatomic lattice. It has been shown that the cutoff modes in nonlinear lattices may have strong interactions. Based on a quasi-discreteness approach we have derived the nonlinear amplitude equations for two coupled cutoff modes and found that a novel class of nonlinearly coupled localized structures in lattices is possible through a cross-phase modulation. The exact solutions in the form of soliton–soliton and kink–soliton pairs of the nonlinear amplitude equations have been given and a modulational stability analysis for two-cutoff-mode excitations has been made. The results have also been checked by numerical simulations. Finally, a pendulum lattice experiment for observing the coupled nonlinearly coupled localized structures has also been suggested.

We should point out that the existence of the nonlinearly coupled localized excitations described above is a common property of discrete nonlinear systems. Thus the theory of the dynamics of coupled cutoff modes developed above is rather general and can be extended to

multi-atomic and higher-dimensional lattices. For the system with N coupled cutoff modes one can obtain the following coupled NLS equations

$$\mathrm{i}\partial A_j/\partial\tau + \Gamma_j\partial^2 A_j/\partial\xi_n^2 + \left(\sum_{l=1}^{N}\Delta_{jl}|A_l|^2\right)A_j = 0 \tag{45}$$

($j = 1, 2, \ldots, N$), where A_j is the envelope of the jth cutoff mode, $\Gamma_j = \omega''(q_j)/2$, Δ_{jl} is the coefficient of the self-phase modulation (for $l = j$) and the cross-phase modulation (for $l \neq j$). The analysis of the system (45) and corresponding nonlinear localized excitations as well as an application to the study of the intrinsic resonant modes in a diatomic lattice with the nearest- and second-neighbour interactions [20] will be presented elsewhere.

Acknowledgments

The discussions with the members at the Centre for Nonlinear Studies of Hong Kong Baptist University are helpful and fruitful. This work was supported by grants from the Hong Kong Research Grants Council, the Hong Kong Baptist University, the Natural Science Foundation of China, and the Development Foundation for Science and Technology of ECNU.

References

[1] Maradudin A A, Montroll E W, Weiss G H and Ipatova I P 1971 *Theory of Lattice Dynamics in the Harmonic Approximation* (New York: Academic)
[2] Fermi E, Pasta J and Ulam S 1962 *Los Alamos National Laboratory Report* LA1940 (also in *Collected Papers of Ernico Fermi* (Chicago, IL: University of Chicago Press) p 978)
[3] Zabusky N J and Kruskal M D 1965 *Phys. Rev. Lett.* **15** 240
[4] Sivers A J and Takeno S 1988 *Phys. Rev. Lett.* **61** 970
[5] Sievers A J and Page J B 1995 *Dynamical Properties of Solids* ed G K Horton and A A Maradudin (Amsterdam: Elsevier) p 137 and references therein
[6] Flach S and Wills C R 1998 *Phys. Rep.* **295** 181 and references therein
[7] Kiselev S A, Bickham S R and Sievers A J 1993 *Phys. Rev.* B **48** 13 508
[8] Bonart D, Rössler T and Page J B 1997 *Phys. Rev.* B **55** 8829
[9] Huang Guoxiang 1995 *Phys. Rev.* B **51** 12 347
[10] Huang Guoxiang and Hu Bambi 1998 *Phys. Rev.* B **57** 5746
[11] Chen Wei-zhong 1994 *Phys. Rev.* B **49** 15 063
[12] Lou Sen-yue and Huang Guoxiang 1995 *Mod. Phys. Lett.* **9** 1231
[13] Marquié P, Bilbault J M and Remoissenet M 1995 *Phys. Rev.* E **51** 6127
[14] Kivshar Y S, Haelterman M and Sheppard A P 1994 *Phys. Rev.* E **50** 3161
[15] Stuart J T and DiPrima R C 1978 *Proc. R. Soc.* A **362** 27
[16] Cross M C and Hohenberg P C 1993 *Rev. Mod. Phys.* **65** 851
[17] Berkhoer A L and Zakharov V E 1970 *Sov. Phys.–JETP* **31** 486
[18] Argrawal G P 1987 *Phys. Rev. Lett.* **59** 880
[19] Denardo B, Galvin G, Greenfield A, Larraza A, Putterman S and Wright W 1992 *Phys. Rev. Lett.* **68** 1730
[20] Kiselev S A, Lai R and Sievers A J 1998 *Phys. Rev.* B **57** 3402